

## Structure of cytoplasmic ring of nuclear pore complex by integrative cryo-EM and AlphaFold

Pietro Fontana Ying Dong Xiong Pi Alexander B. Tong Corey W. Hecksel Longfei Wang Tian-Min Fu Carlos Bustamante Hao Wu

*Science*, 376 (6598), eabm9326. • DOI: 10.1126/science.abm9326

### View the article online

<https://www.science.org/doi/10.1126/science.abm9326>

### Permissions

<https://www.science.org/help/reprints-and-permissions>

Use of this article is subject to the [Terms of service](#)

---

*Science* (ISSN ) is published by the American Association for the Advancement of Science. 1200 New York Avenue NW, Washington, DC 20005. The title *Science* is a registered trademark of AAAS.

Copyright © 2022 The Authors, some rights reserved; exclusive licensee American Association for the Advancement of Science. No claim to original U.S. Government Works



## Supplementary Materials for

### **Structure of cytoplasmic ring of nuclear pore complex by integrative cryo-EM and AlphaFold**

Pietro Fontana *et al.*

Corresponding author: Hao Wu, [wu@crystal.harvard.edu](mailto:wu@crystal.harvard.edu)

*Science* **376**, eabm9326 (2022)

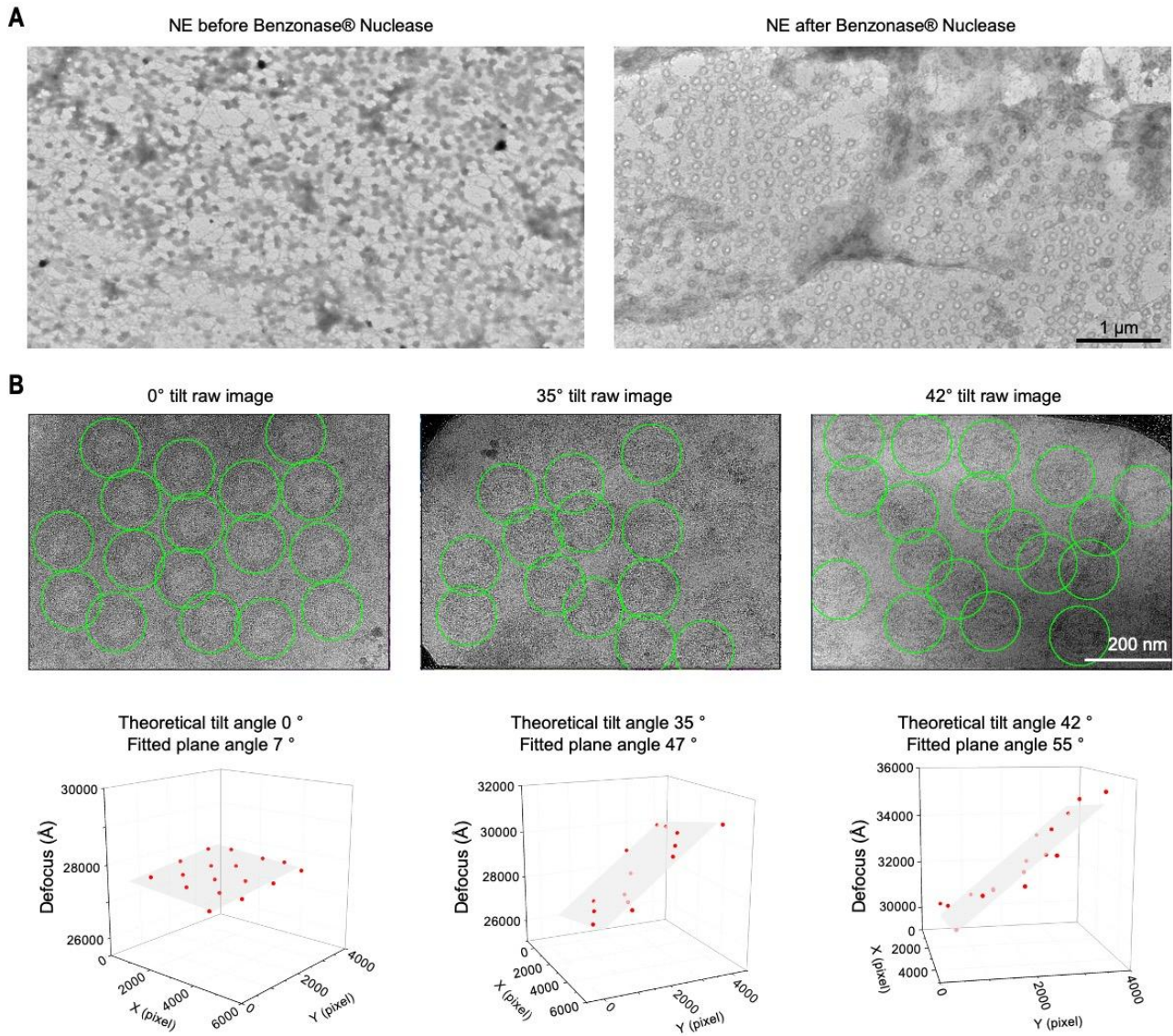
DOI: [10.1126/science.abm9326](https://doi.org/10.1126/science.abm9326)

#### **The PDF file includes:**

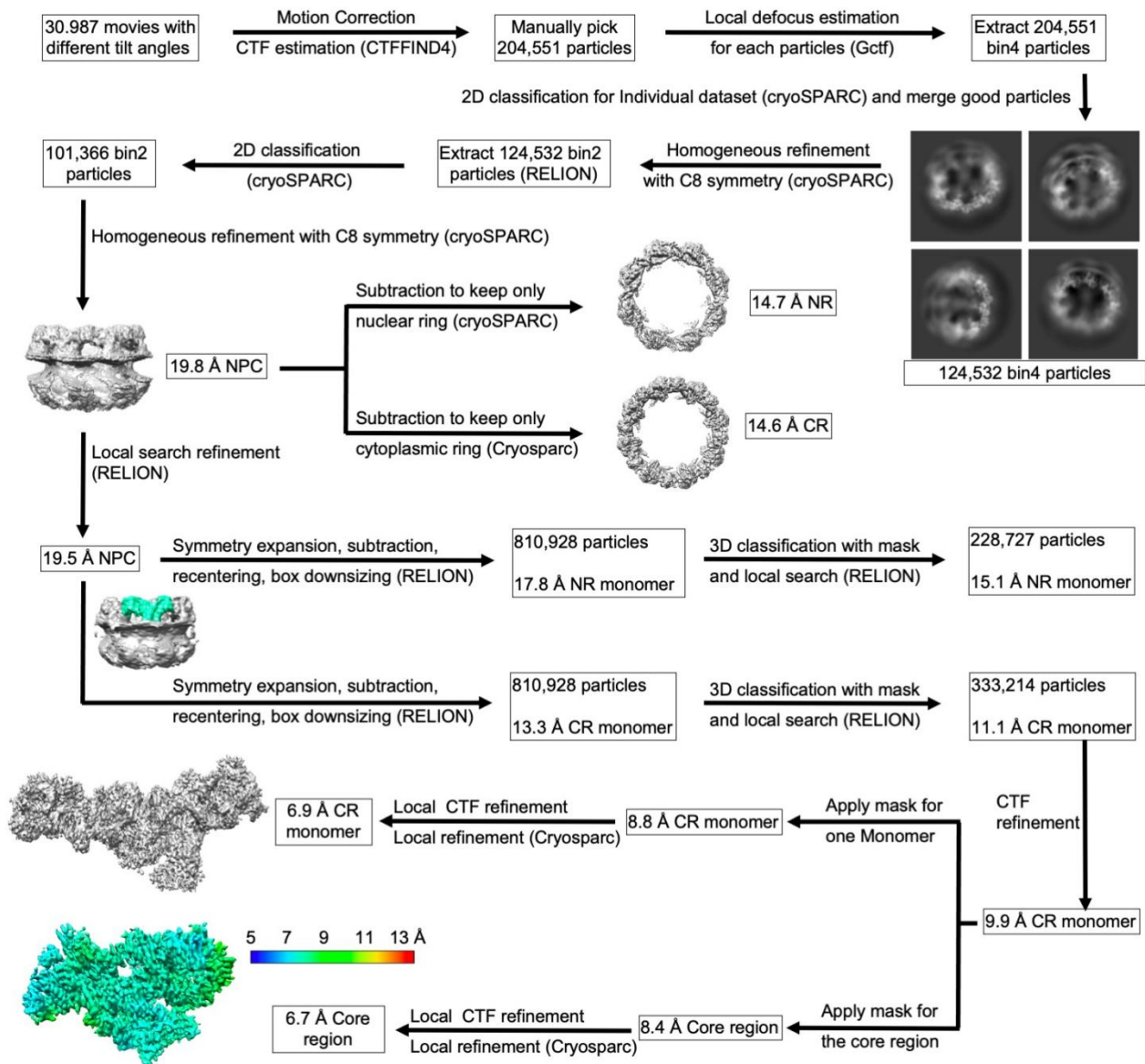
Figs. S1 to S8  
Tables S1 to S6

#### **Other Supplementary Material for this manuscript includes the following:**

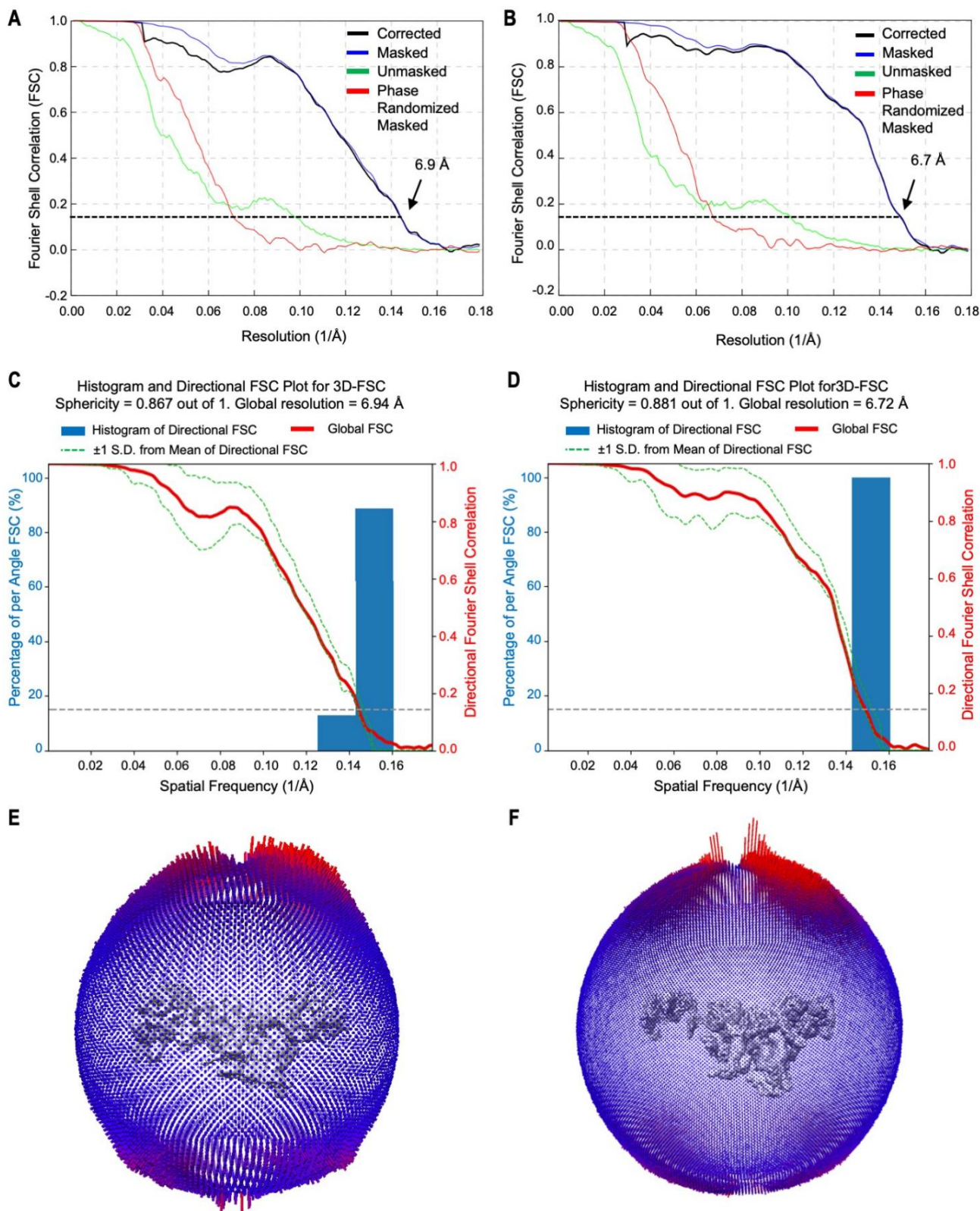
MDAR Reproducibility Checklist



**Fig. S1. Sample preparation and cryo-EM data quality.** (A) A representative negative staining EM image of the nuclear envelope (NE) before (left) and after (right) treatment with Benzonase® Nuclease. (B) Raw cryo-EM images (top) and 3D plots composed of the X and Y positions and the defocus levels ( $\Delta Z$ ) of the particles in tilt images (bottom). Planes that fit the data points are shown.



**Fig. S2. Cryo-EM data processing flow chart and local resolution.**

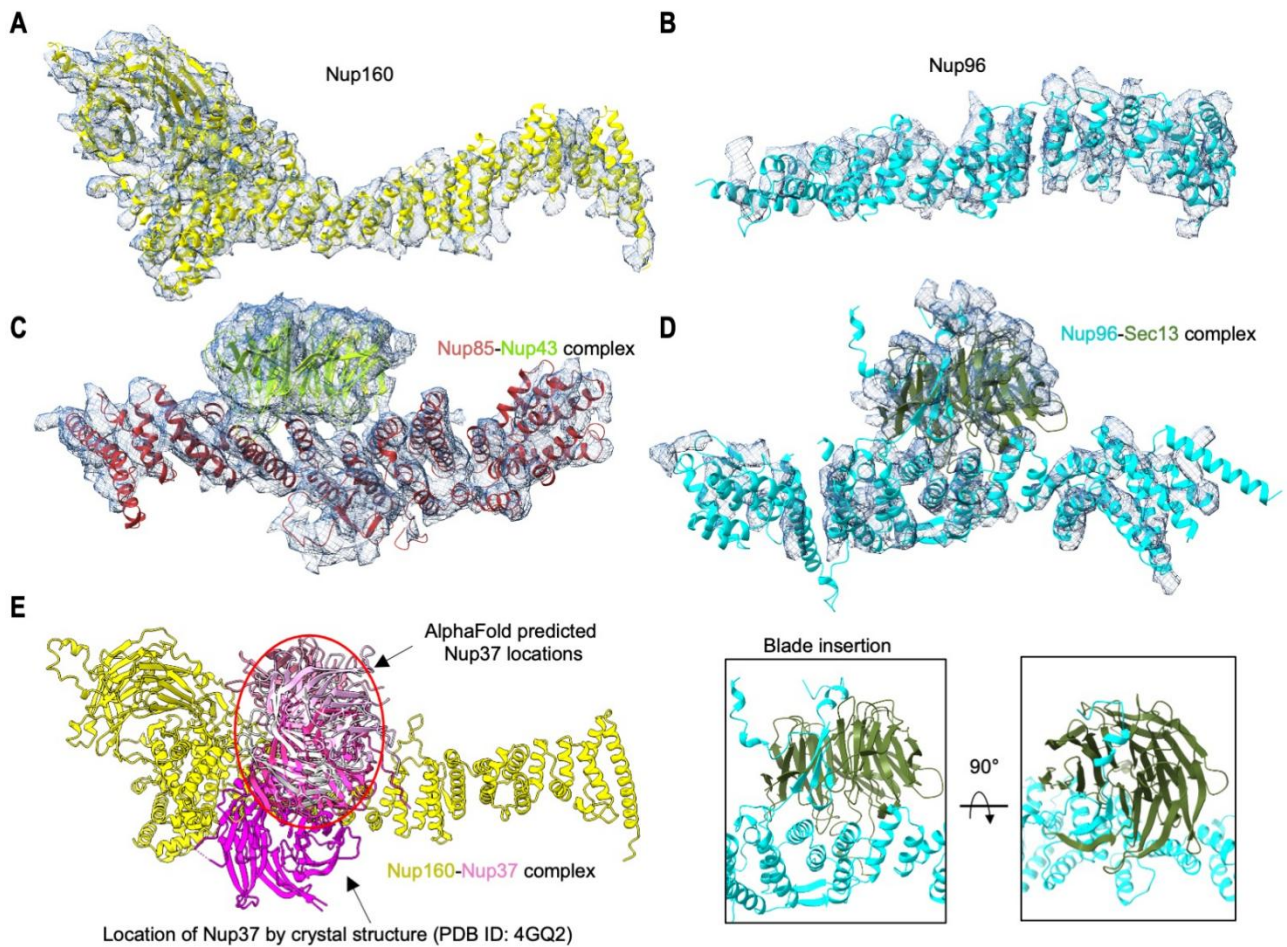


**Fig. S3. The quality of cryo-EM maps for the cytoplasmic ring (CR). (A-B)** Fourier shell correlation plots for the CR protomer (A) and the core region (B). **(C-D)** Directional FSC plots for the CR protomer (C) and the core region (D). **(E-F)** Angular distribution of the particles used for the final reconstruction of the CR protomer (E) and the core region (F).

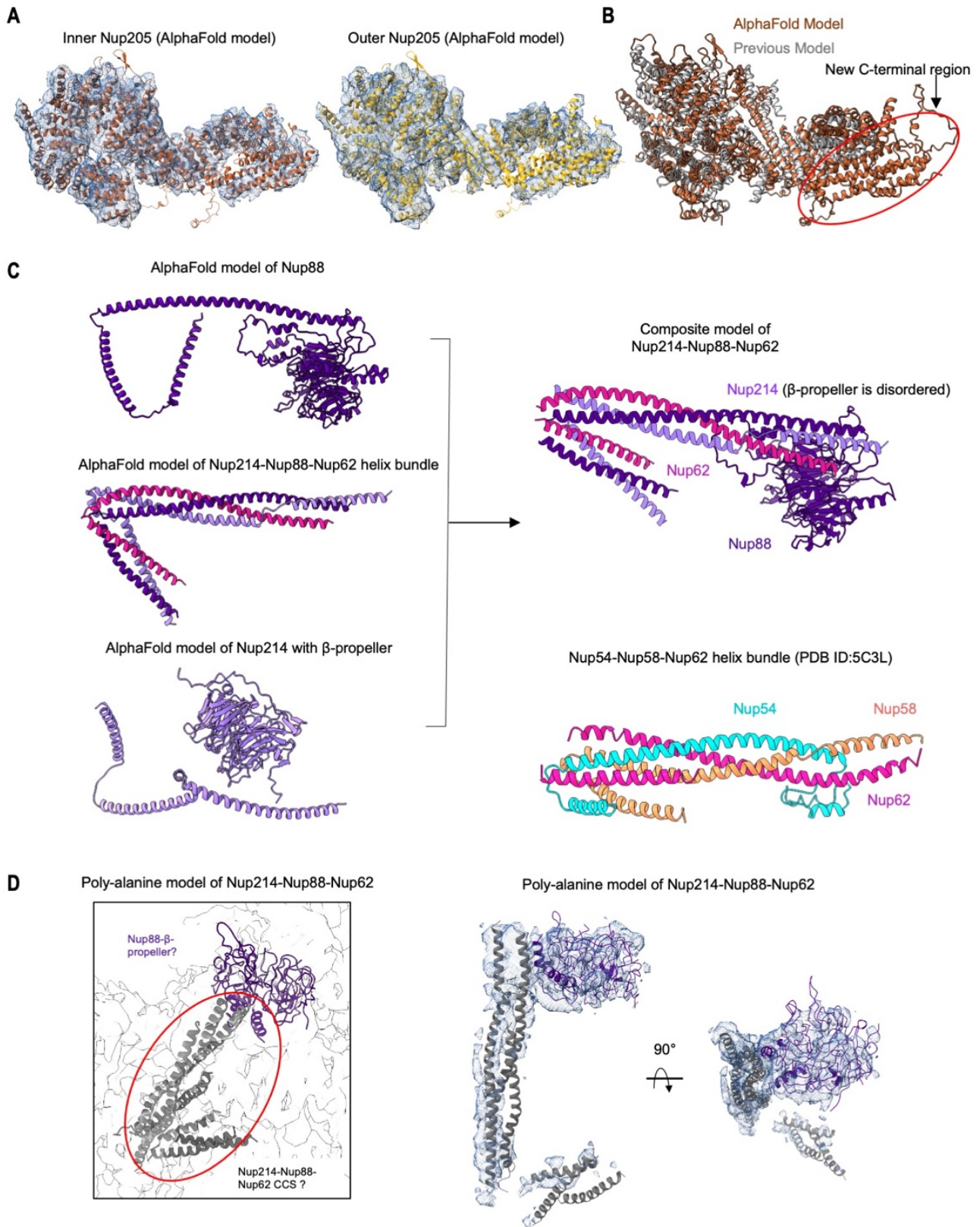
AlphaFold logical flow

- Predict structures of individual Nups, look at the agreement among models, and pick the top ranked, or consensus models.
- For helical Nups, fit to density by prominent helical features.
- For  $\beta$ -propeller Nups, predict complex structures with contacting helical Nups, and confirm density positioning.
- For ambiguous Nup interactions, predict binary complex structures, and confirm density positioning.

**Fig. S4. AlphaFold flow chart.**



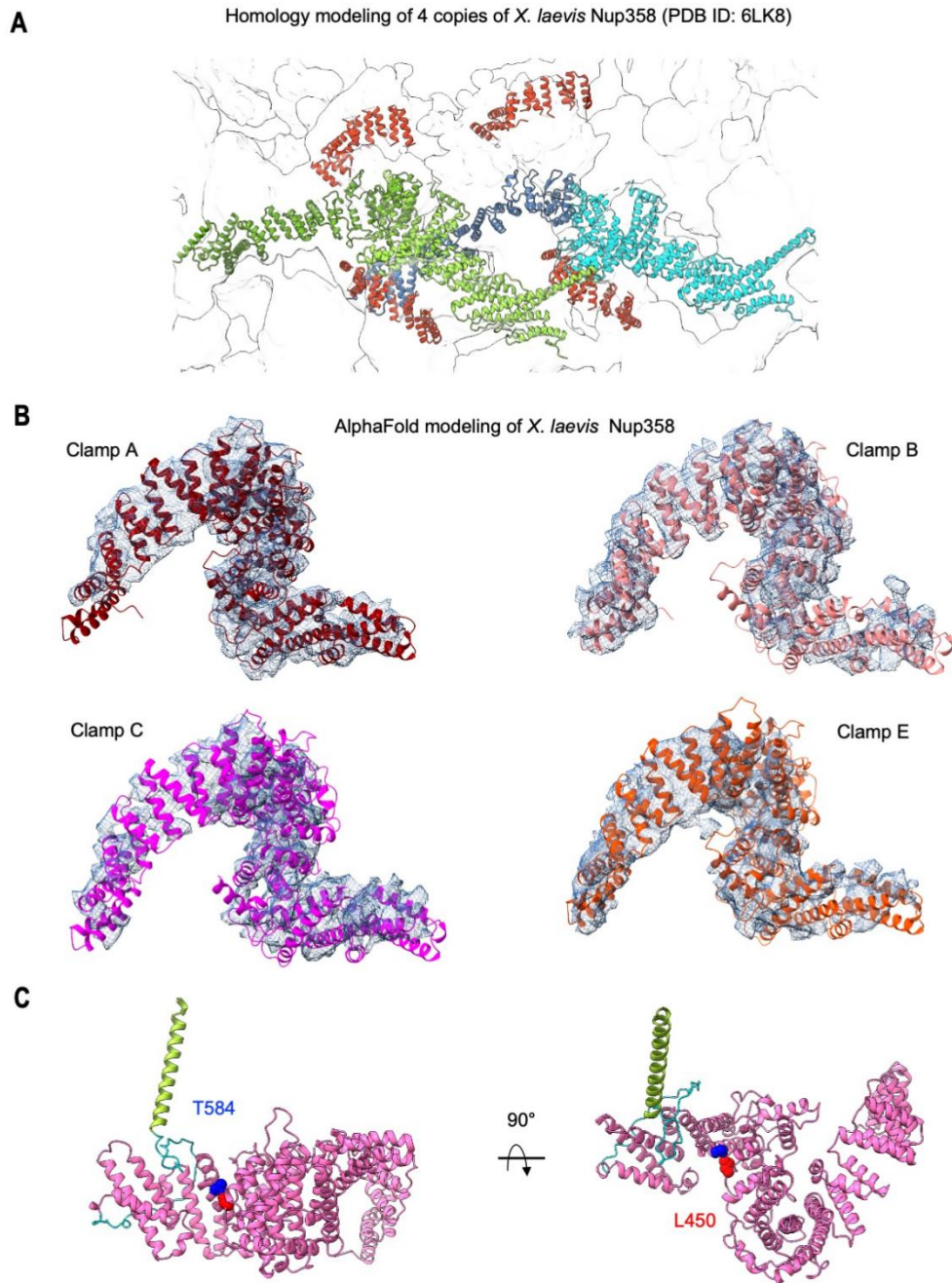
**Fig. S5. Cryo-EM map fitting of predicted structures of Nups in the Y-complex.** (A-C) Predicted Nup160 (A), Nup96 (B) and the Nup85-Nup43 complex (C) structures fitted in the map (contour level:  $4.5 \sigma$ ), showing alignment of the  $\alpha$ -helical features. (D) Predicted Nup96-Sec13 complex structures fitted in the map (top, contour level:  $4.5 \sigma$ ) and details at the location of blade insertion of the  $\beta$ -propeller domain (bottom). (E) AlphaFold failed to predict the Nup37-Nup160 complex structure.



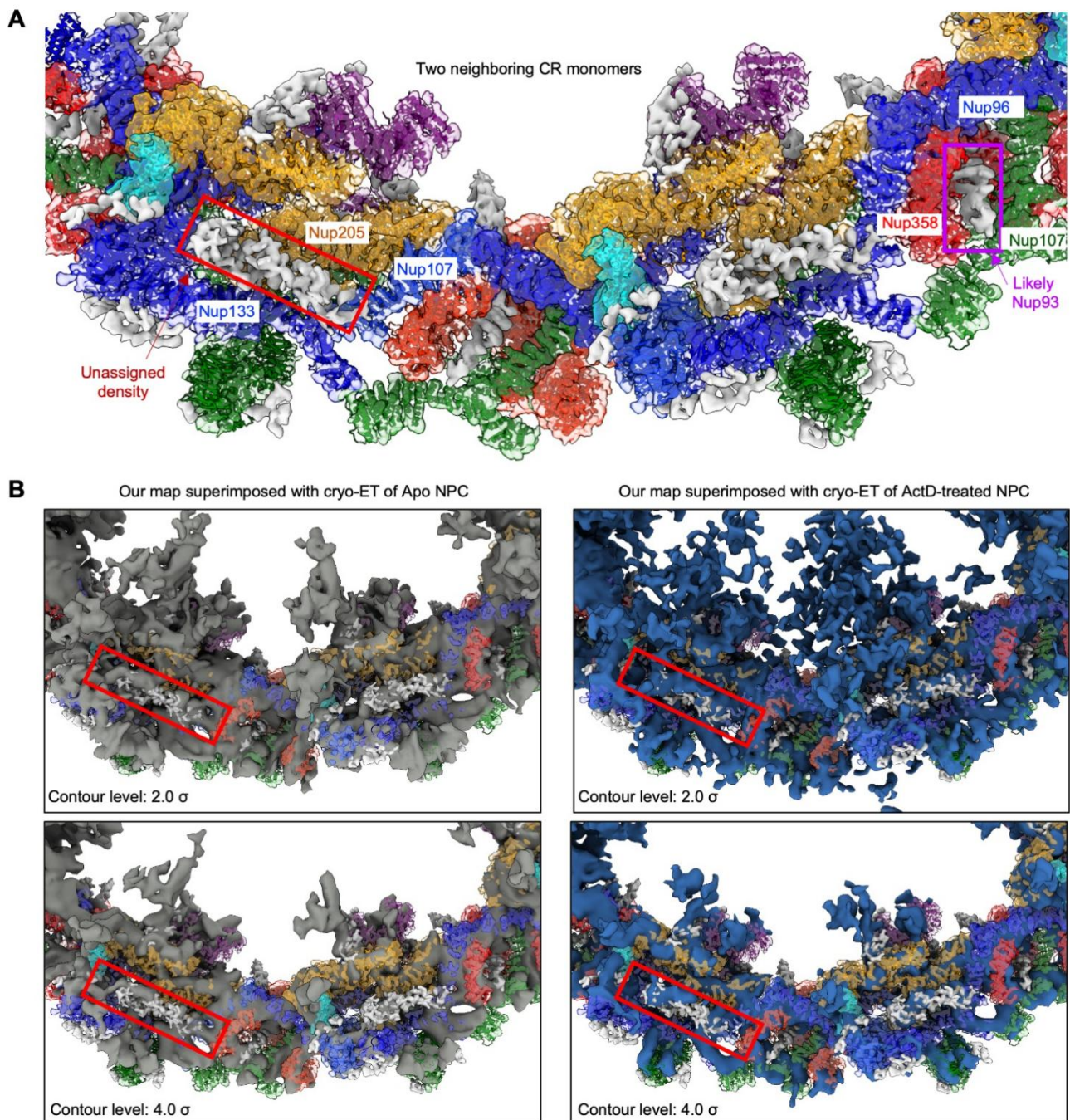
**Fig. S6. Fitting of Nup205 and the Nup214-Nup88-Nup62 complex.** (A) AlphaFold-generated model of Nup205 fitted into cryo-EM densities (contour level:  $4.5 \sigma$ ) near inner and outer Y-complexes. (B) Superimposed Nup205 models from AlphaFold (orange) and from homology model (gray, PDB ID: 6KL8). AlphaFold model shows a



previously missing C-terminal region. **(C)** Generation of the Nup214-Nup88-Nup62 composite model by combining multiple AlphaFold Predictions; each Nup was first predicted independently followed by prediction of the hetero-trimeric coiled coil bundles. Fitting of the composite model (top right) to the cryo-EM density is shown in Figure 3C. The homologous *X. laevis* Nup54-Nup58-Nup62 helix bundle structure (lower right) is shown for comparison. **(D)** Previously published poly-alanine model from PDB ID: 6KL8 fitted into the Nup214-Nup88-Nup62 density (contour level:  $4.5 \sigma$ ). The shorter trimeric coiled coil is out of our density.



**Fig. S7. Nup358 model and fitting.** (A) *X. laevis* Nup358 generated by homology modeling from 4GA0 (PDB ID: 6KL8). (B) Nup385 model generated by AlphaFold fitted into the cryo-EM density map (contour level:  $8.0 \sigma$ ; density for clamp D is shown in Figure 4C). (C) Partially buried residue T584 (blue, Human T585) associated with autosomal dominant acute necrotizing encephalopathy (ADANE) interacts with L450 (red), and the T584M mutation may affect the structure.



**Fig. S8. Unassigned densities in the *X. laevis* NPC CR map.** (A) Cryo-EM density map (contour level: 4.5  $\sigma$ ) of two neighboring CR protomers with all the assigned densities colored individually; Two dominant unassigned pieces of density are shown in light gray, and boxed in red and magenta respectively. One of them (boxed in magenta) should correspond to Nup93 but we cannot reliably fit our Nup93 model into the density. (B) Cryo-EM density map superimposed with *X. laevis* NPC cryo-ET map (EMDB:3005 and EMDB:3009) at lower and higher contour levels showing the existence of the red-boxed density. Left panel: Apo map (EMDB:3005) colored in dark gray; Right panel, ActD-treated map (EMDB:3009), colored in dark blue.

**Table S1. Data Collection, data processing and validation statistics**

NPC CR protomer (EMD-25817) and composite full ring (EMD-25818) at 6.9 Å resolution

**Data Collection and Processing (for each dataset)**

Microscope	Titan Krios
Voltage (keV)	300
Camera	K3
Magnification	64,000
Pixel size at detector (Å/pixel)	1.4
Total electron exposure (e <sup>-</sup> /Å <sup>2</sup> )	80 to 140
Exposure rate (e <sup>-</sup> /pixel/sec)	1 to 1.4
Number of frames collected during exposure	80 to 140
Defocus range (µm)	-1 to -3
Automation software (EPU, SerialEM or manual)	SerialEM
Tilt angle (if grid was tilted, in degrees)	0, 35, 42, 45
Energy filter slit width (if used, in eV)	20
Micrographs collected (no.)	45,278
Micrographs used (no.)	30,987
Total extracted particles (no.)	204,551

**Each Reconstruction after Symmetry Expansion**

Refined particles (no.) / Final particles (no.)	333,214 / 333,214
Point-group or helical symmetry parameters	
Estimated error of translations/rotations (if available)	
Resolution (global, Å)	6.9
FSC 0.5 (unmasked / masked)	25 / 9.1
FSC 0.143 (unmasked / masked)	10.2 / 6.9
Resolution range (local, Å)	5.5 to 10
Resolution range due to anisotropy (Å)	6.0 to 9.1
Map sharpening <i>B</i> factor range (Å <sup>2</sup> )	-503 to -710
Map sharpening methods	LocalDeblur

**Model composition (for each model)**


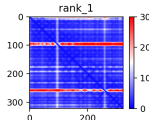
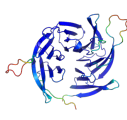
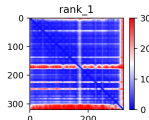
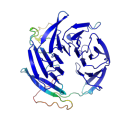
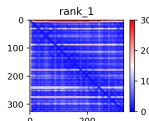
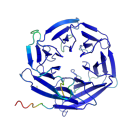
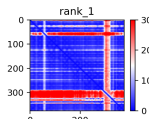
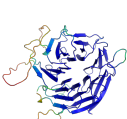
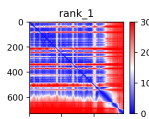
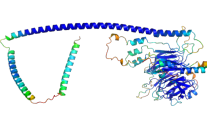
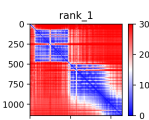
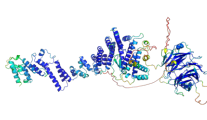
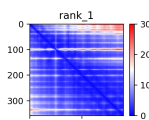
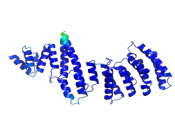
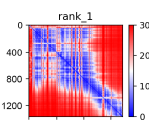
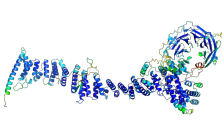
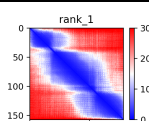
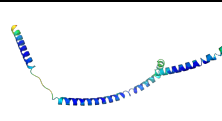
Protein residues	21,112
------------------	--------

**Validation (for each model)**


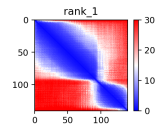
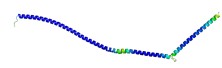
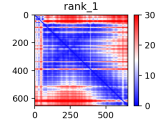
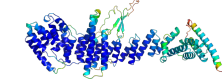
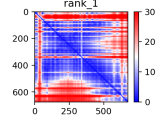
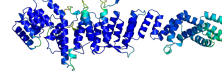
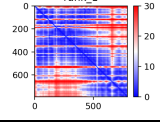
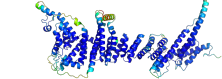
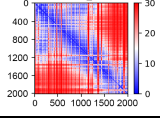
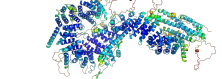
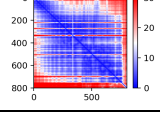
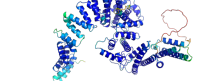
Model-Map scores	
CC (Chimera, Phenix)	0.69, 0.63
Average FSC (0 / 0.143 / 0.5)	(7.6 / 9.7 / 27.1)
R.m.s. deviations from ideal values	
Bond lengths (Å)	0.012
Bond angles (°)	1.778
MolProbity score	2.13
CaBLAM outliers	1.18
Clashscore	20.05
Poor rotamers (%)	0.88
C-beta outliers (%)	0.23
Ramachandran plot	
Favored (%)	95.2
Outliers (%)	1.32

**Table S2. Statistics on AlphaFold-predicted  $\beta$ -propeller-containing single Nups.**


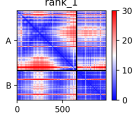
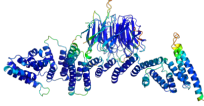
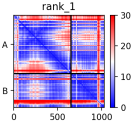
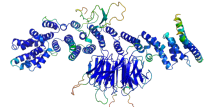
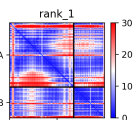
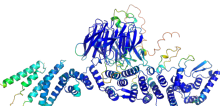
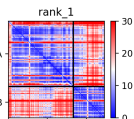
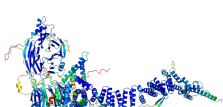
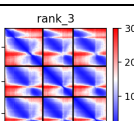
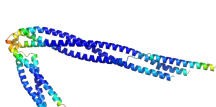
For each Nup, pLDDT (predicted local distance difference test), pTM (predicted template modeling), RMSD (root-mean-square deviation) range for pairwise superposition between rank 2-5 models and rank 1 model, fitting CC (correlation coefficient) of rank 1 model into the cryo-EM density, predicted alignment error (PAE) matrix, and ribbon diagram colored by per-residue pLDDT are shown. Residues predicted with high pLDDT or high confidence are in blue.

		PAE	Per-residue pLDDT 
Seh1	pLDDT: 92.1, pTM 0.90 RMSD: 0.14 to 0.22 ChimerX Fitting CC: 0.85 Phenix Fitting CC: 0.8		
Sec13	pLDDT: 88.8, pTM 0.87 RMSD: 0.12 to 0.16 ChimerX Fitting CC: 0.88 Phenix Fitting CC: 0.8		
Nup37	pLDDT: 92.0, pTM 0.89 RMSD: 0.15 to 0.22 ChimerX Fitting CC: 0.89 Phenix Fitting CC: 0.63		
Nup43	pLDDT: 86.5, pTM 0.86 RMSD: 0.12 to 0.17 ChimerX Fitting CC: 0.86 Phenix Fitting CC: 0.82		
Nup88	pLDDT: 80.1, pTM 0.74 RMSD: 0.48 to 1.6 ChimerX Fitting CC: 0.88 Phenix Fitting CC: 0.65		
Nup133	pLDDT: 79.8, pTM 0.53 RMSD: $\beta$ 0.17 to 0.12, $\alpha$ 0.7 to 1 ChimerX Fitting CC: 0.82 Phenix Fitting CC: 0.57		
Nup155 (aa 1031-1388)	pLDDT: 93, pTM 0.86 RMSD: 0.33 to 0.45 ChimerX Fitting CC: 0.79 Phenix Fitting CC: 0.66		
Nup160	pLDDT: 78.6, pTM 0.67 RMSD: 0.93 to 1.8 ChimerX Fitting CC: 0.85 Phenix Fitting CC: 0.5		
Nup214 (aa 697-853)	pLDDT: 0.93 pTM 0.43 RMSD: 1.26 to 3.4 ChimerX Fitting CC: 0.86 Phenix Fitting CC: 0.55		

**Table S3. Statistics on AlphaFold-predicted all helical single Nups.** For each Nup, pLDDT (predicted local distance difference test), pTM (predicted template modeling), RMSD (root-mean-square deviation) range for pairwise superposition between rank 2-5 models and rank 1 model, fitting CC (correlation coefficient) of rank 1 model into the cryo-EM density, predicted alignment error (PAE) matrix, and ribbon diagram colored by per-residue pLDDT are shown. Residues predicted with high pLDDT or high confidence are in blue.

		PAE	Per-residue pLDDT 
Nup62 (aa 350-490)	pLDDT: 91.4, pMT 0.47 RMSD: 0.75 to 1.1 ChimerX Fitting CC: 0.79 Phenix Fitting CC: 0.46		
Nup85	pLDDT: 86.3, pTM 0.78 RMSD: 0.42 to 0.49 ChimerX Fitting CC: 0.75 Phenix Fitting CC: 0.7		
Nup96 (aa 250-923)	pLDDT: 68.4, pTM 0.7 RMSD: 0.5 to 1.13 ChimerX Fitting CC: 0.84 Phenix Fitting CC: 0.69		
Nup107 (aa 117-905)	pLDDT: 86.4, pTM 0.79 RMSD: 0.4 to 0.58 ChimerX Fitting CC: 0.81 Phenix Fitting CC: 0.62		
Nup205	pLDDT: 78.3, pTM 0.74 RMSD: 1.04 to 1.77 ChimerX Fitting CC: 0.88 Phenix Fitting CC: 0.69		
Nup358 (aa 1-800)	pLDDT: 86.2, pTM 0.81 RMSD: 0.26 to 0.41 ChimerX Fitting CC: 0.8 Phenix Fitting CC: 0.68		

**Table S4. Statistics on AlphaFold-predicted Nup complexes.** For each complex, pLDDT (predicted local distance difference test), pTM (predicted template modeling), RMSD (root-mean-square deviation) range for pairwise superposition between rank 2-5 models and rank 1 model, fitting CC (correlation coefficient) of rank 1 model into the cryo-EM density, predicted alignment error (PAE) matrix, and ribbon diagram colored by per-residue pLDDT are shown. Residues predicted with high pLDDT or high confidence are in blue.


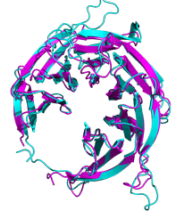
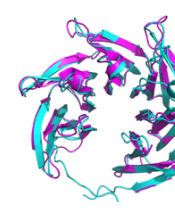
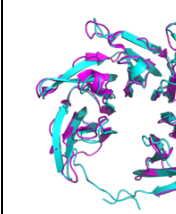
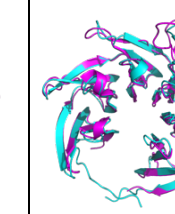
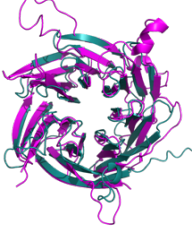
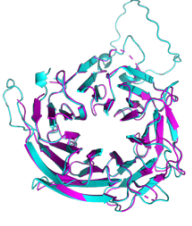
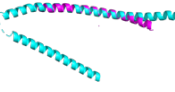
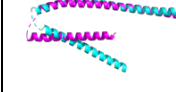
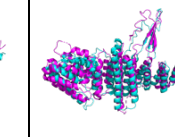
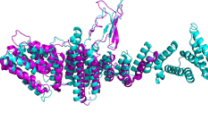
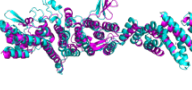

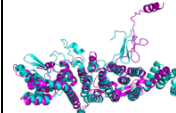
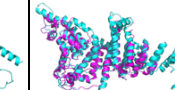
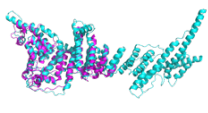
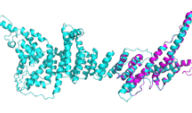
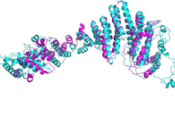
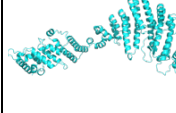

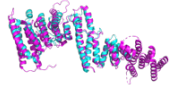
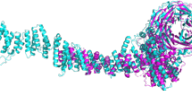
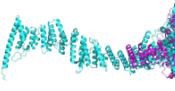
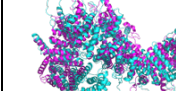
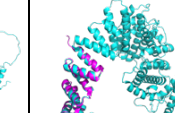
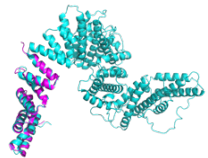
		PAE	Per-residue pLDDT 
Nup85(A)-Seh1(B)	pLDDT: 87.18, pTM 0.82 RMSD: 0.46 to 0.63 Fitting CC: 0.83		
Nup85(B)-Nup43(A)	pLDDT: 85.1, pTM 0.82 RMSD: 0.4 to 0.68 Fitting CC: 0.84		
Nup96(aa 250-923)(A)- Sec13(B)	pLDDT: 83.52, pTM 0.83 RMSD: 0.38 to 0.58 Fitting CC: 0.82		
Nup160(A)-Nup133(B)	pLDDT: 80.15, pTM 0.76 RMSD: Rank 1-5 1.1, Rank 2-3-4 0.74 Fitting CC: 0.85		
Nup214(A)-Nup88(B)- Nup62(C) hetero- trimeric (Rank 3)	pLDDT: 87.5, pTM 0.6 RMSD: 0.88 to 1.4 Fitting CC: 0.84		

**Table S5. AlphaFold-predicted model and their PDB homologs.** For each *Xenopus laevis* Nup, its total amino acid length, the number of residues built by AlphaFold, close homologs in the PDB and their species, amino acid length of the PDB structures, RMSD (root-mean-square deviation) of the PDB structure against the AlphaFold model, and % identity of homologous PDB structures against the *Xenopus Laevis* sequence. Xi: *Xenopus laevis*; Sc: *Saccharomyces cerevisiae*; Sp: *Schizosaccharomyces pombe*; Hs: *Homo sapiens*; Rt: *Rattus norvegicus*; Ct: *Chaetomium thermophilum*; Pg: *Pan troglodytes*. Nups highlighted in red have only partial PDB structures of their homologs. NA: sequence homology below detection.

<b>X. laevis Nup</b>	<b>Total length (aa)</b>	<b>Ordered and built by AlphaFold (aa)</b>	<b>Homolog in PDB</b>	<b>PDB length (aa)</b>	<b>RMSD</b>	<b>Identity (%)</b>
<b>Seh1</b>	360	322	4XMM Sc	349	0.946	34.38
			3F3F Sc	351	0.896	34.38
<b>Sec13</b>	360	306	4XMM Sc	297	0.87	49.83
			3IKO Sc	297	0.899	49.83
			3BG1 Sc	316	0.663	88.61
<b>Nup37</b>	326	326	4GQ2 Sp	393	3.547	27.56
<b>Nup43</b>	375	375	4I79 Hs	380	0.427	67.81
<b>Nup62</b>	547	A 130, B 28	5H1X Rn	52	2.98	86.54
			5C3L XI	150	1.287	100.00
<b>Nup85</b>	653	653	4XMM Sc	701	6.676	22.28
			3F3F Sc	570	9.476	22.28
<b>Nup96</b>	923	638	4XMM Sc	647	6.015	21.12
			3IKO Sc	427	3.824	21.12
			3BG1 Sc	431	4.071	21.12
<b>Nup107</b>	916	789	4XMM Sc	451	3.916	24.32
			3IKO Sc	460	3.894	23.73
			3I4R Hs	277	0.666	83.96
<b>Nup133</b>	1140	Inner 1064, Outer 670	3I4R Hs	644	6.726	71.03
			1XKS Hs	450	0.712	56.81
<b>Nup155</b>	1388	357	5HB1 Ct	830	6.859	25.3
			5HAZ Ct	567	5.155	28.57
<b>Nup160</b>	1435	1350	4XMM Sc	1036	15.798	NA
			4GQ2 Sp	950	14.83	NA
<b>Nup205</b>	2011	2011	5HB4 Ct	1596	6.525	23.66
<b>Nup358</b>	2905	798	4GA0 Hs	150	0.84	68.75
			4GA2 Pg	150	0.7	68.06



**Table S6. AlphaFold-predicted model aligned with their PDB homologs.** Each *Xenopus leavis* Nup predicted by AlphaFold (cyan) were aligned with available PDB homologs (magenta). RMSD and identity for all the alignment are reported in Table S5.

				
Seh1 - 4XMM	Seh1 - 3F3F	Sec13 - 4XMM	Sec13 - 3IKO	Sec13 - 3BG1
				
Nup37 - 4GQ2	Nup43 - 4I79	Nup62 - 5H1X	Nup62 - 5C3L	Nup85 - 4XMM
				
Nup85 - 3F3F	Nup96 - 4XMM	Nup96 - 3IKO	Nup96 - 3BGI	Nup107 - 4XMM
				
Nup107 - 3IKO	Nup107 - 3I4R	Nup133 - 3I4R	Nup133 - 1XKS	Nup155 - 5HB1
				
Nup155 - 5HAZ	Nup160 - 4XMM	Nup160 - 4GQ2	Nup205 - 5HB4	Nup358 - 4GA0
				
Nup358 - 4GA2				